A modelling approach to study the fouling of an anaerobic membrane bioreactor for industrial wastewater treatment

Amine Charfi, Narumol Thongmak, Boumediene Benyahia, Muhammad Aslam, Jérôme Harmand, Nihel Ben Amar, Geoffroy Lesage, Porntip Sridang, Jeonghwan Kim, Marc Héran

HAL Id: hal-01670209

https://hal.umontpellier.fr/hal-01670209v1

Submitted on 2 Jun 2021

Accepted Manuscript

A modelling approach to study the fouling of an Anaerobic Membrane Bioreactor for industrial wastewater treatment

Amine Charfi, Narumol Thongmak, Boumediene Benyahia, Muhammad Aslam, Jérôme Harmand, Nihel Ben Amar, Geoffroy Lesage, Porntip Sridang, Jeonghwan Kim, Marc Heran

Please cite this article as: Charfi, A., Thongmak, N., Benyahia, B., Aslam, M., Harmand, J., Amar, N.B., Lesage, G., Sridang, P., Kim, J., Heran, M., A modelling approach to study the fouling of an Anaerobic Membrane Bioreactor for industrial wastewater treatment, *Bioresource Technology* (2017), doi: http://dx.doi.org/10.1016/j.biortech. 2017.08.003

A modelling approach to study the fouling of an Anaerobic Membrane Bioreactor for industrial wastewater treatment

Amine Charfi[a], Narumol Thongmak[b], Boumediene Benyahia[c], Muhammad Aslam[a], Jérôme Harmand[d], Nihel Ben Amar[e], Geoffroy Lesage[f], Porntip Sridang[g], Jeonghwan Kim[a], Marc Heran[f]

[a] Department of Environmental Engineering, Inha University, Namgu Yonghyun dong 253, Incheon, Republic of Korea

[b] Environmental Science Program, Faculty of Science Technology and Agriculture, Yala Rajabhat University, Muang, Yala 95000, Thailand, Center of Excellence on Hazardous Substance Management (HSM), Bangkok 10330, Thailand

[c] Control Laboratory of Tlemcen, University of Tlemcen, B.P. 230, Tlemcen 13000, Algeria

[d] LBE, INRA, 11100, Narbonne, France

[e] Université de Tunis El Manar, Ecole Nationale des Ingénieurs de Tunis, ENIT Laboratoire de Modélisation Mathématique et Numérique dans les Sciences de L'Ingénieur, LAMSIN, Tunisia

[f] Institut Européen des Membranes, IEM, UMR-5635, Université de Montpellier, ENSCM, CNRS, Place Eugène Bataillon, 34095 Montpellier cedex 5, France

[g] Department of Environmental Science, Faculty of Science, Silpakorn University, Muang, Nakhonpathom 73000, Thailand, Center of Excellence on Hazardous Substance Management (HSM), Bangkok 10330, Thailand

*corresponding author: amine.charfi@ymail.com,

E-mail adresses : amine.charfi@ymail.com (A. Charfi), mind.of.my@gmail.com (N.Thongmak) b.benyahia.ut1@gmail.com (B. Benyahia), maslam@ciitlahore.edu.pk (M. Aslam), jerome.harmand@inra.fr (J. Harmand), benamar_nihel@yahoo.fr (N. Ben Amar) , geoffroy.lesage@umontpellier.fr (G. Lesage), porntipsridang999@gmail.com (P.Sridang), jeonghwankim@inha.ac.kr (J. Kim), heran@um2.fr (M. Heran).

Nomenclature

A	: membrane surface area (m^2)	R_0	: intrinsic membrane resistance (m^{-1})
b	: S_2 yield from SMP (-)	S_1	: COD concentration ($kgCOD.m^{-3}$)
b_1	: SMP yield from S_1 (-)	S_2	: VFA concentration ($kg_{equivalent\ acetate}.m^{-3}$)
b_2	: SMP degradation by X_1 (-)	S	: SMP concentration ($kg.m^{-3}$)
b_3	: SMP yield from S_2 (-)	TMP	: transmembrane pressure (Pa)
d	: cake particle diameter (m)	V_R	: reactor volume (m^3)
k_1^*	: yield for S_1 degradation (-)	V_c	: cake volume (m^3)
k_2^*	: yield for S_2 production (-)	V_s	: volume of SMP trapped in cake (m^3)
k_3^*	: yield for S_2 consumption (-)	X_1	: Acidogens concentration ($kg.m^{-3}$)
k_4^*	: yield for CO_2 production (L/g_{COD})	X_2	: Methanogens concentration ($kg.m^{-3}$)
k_5^*	: yield for CO_2 production (L/g_{COD})	X_{TSS}	: Total Suspended Solid ($kg.m^{-3}$)
k_6^*	: yield for CH_4 production (L/g_{COD})	α	: specific cake resistance ($m.kg^{-1}$)
K1	: half saturation constant ($kg.m^{-3}$)	β	: shear parameter (kg^{-1})
K2	: half saturation constant ($kg.m^{-3}$)	ε	: cake porosity
Ki	: inhibition constant ($kg.m^{-3}$)	$ε_0$	: initial cake porosity
K	: half saturation constant ($kg.m^{-3}$)	$ρ_c$	: cake density ($kg.m^{-3}$)
k_{d1}	: acidogens decay rate (d^{-1})	$ρ_{smp}$	: SMP density ($kg.m^{-3}$)
k_{d2}	: methanogens decay rate (d^{-1})	$μ_p$	: permeate viscosity (Pa.s)
$k_ε$	: coefficient of cake porosity decrease	$μ_1$	: growth rate of acidogens by consuming organic matter (d^{-1})
m_c	: Cake mass (kg)	$μ_2$	: growth rate of methanogens by consuming VFA (d^{-1})
m_X	: Specific mass of suspended solids within the cake (kg/m^2)	$μ_{smp}$	: growth rate of acidogens by consuming SMP (d^{-1})
m_s	: Specific mass of SMP within the cake (kg/m^2)	$μ_{max1}$	: maximum growth rate of acidogens by consuming COD (d^{-1})
n	: empirical constant	$μ_{max2}$	: maximum growth rate of methanogens by consuming

VFA (d^{-1})

Q_w : withdraw flow rate ($m^3.s^{-1}$) μ_{max3} :maximum growth rate of acidogens by consuming SMP (d^{-1})

Q_{in} : feed flowrate ($m^3.s^{-1}$) σ : SMP fraction rejected by the membrane (-)

Q_{out} : permeate flow rate ($m^3.s^{-1}$) φ_{CH4} : Methane flowrate ($mol_{CH4}.L^{-1}.day^{-1}$)

R_c : cake resistance (m^{-1})

Abstract

An Anaerobic Membrane BioReactors (AnMBR) model is presented in this paper based on the combination of a simple fouling model and the Anaerobic Model 2b (AM2b) to describe biological and membrane dynamic responses in an AnMBR. In order to enhance the model calibration and validation, Trans-Membrane Pressure (TMP), Total Suspended Solid (TSS), COD, Volatile Fatty Acid (VFA) and methane production were measured. The model shows a satisfactory description of the experimental data with $R^2 \approx 0.9$ for TMP data and $R^2 \approx 0.99$ for biological parameters. This new model is also proposed as a numerical tool to predict the deposit mass composition of suspended solid and Soluble Microbial Products (SMP) on the membrane surface. The effect of SMP deposit on the TMP jump phenomenon is highlighted. This new approach offers interesting perspectives for fouling prediction and the on-line control of an AnMBR process.

Keywords: anaerobic membrane bioreactor, modelling, membrane fouling, biogas production, deposit analysis.

1. Introduction

The Anaerobic Membrane BioReactor (AnMBR) has been proven to be an efficient waste water treatment technology which allows energy recovery from influent (Wang et al. 2013; Xia et al. 2016; Aslam et al. 2017). An AnMBR associates the advantages of the anaerobic

3

reactor able to treat the majority of organic pollutants, and those of the porous membrane bioreactor processes able to dissociate the Sludge Retention Time (SRT) and the Hydraulic Retention Time (HRT). An AnMBR leads, indeed, to a more efficient biological treatment where the totality of the suspended solids are retained in the reactor allowing a lower HRT which increases both process intensification and effluent water quality (Smith et al. 2012). Nevertheless one major drawback still hinders AnMBR performance, which is membrane fouling (Aslam et al. 2014; Aslam et al. 2017; Charfi et al. 2012). The Suspended Solids (SS) and the Soluble Microbial Products (SMP) are usually assumed to be the major factors responsible for fouling in MBRs (Ho and Sung 2009; Pan et al. 2010; Waeger et al. 2010). Each of these foulants involves both different scales of fouling and mechanisms (Meng et al. 2009; Zuthi et al. 2017), which must be thoroughly characterized in order to enhance the membrane life time and the performance of the AnMBR. It is thus necessary to develop a simple modelling tool to (i) better understand the impact of the operating parameters and then (ii) optimize online AnMBR control.

The sole online tool to quantify the fouling intensity is the monitoring of Trans-Membrane Pressure (TMP). The models proposed in the literature are mainly based on the 'resistance in series' model and Darcy's law or coupling the classic blocking laws of Hermia published in 1982 (Abdelrasoul et al. 2013; Charfi et al. 2014; Charfi et al. 2015; Charfi et al. 2017; Wu et al. 2011). These models are purely physical; they describe abiotic parameter variation and neglect the biological dynamics. To obtain more accurate MBR fouling models, integrated models have been established to consider both the biological dynamics and the fouling ones. The combined models have been largely investigated in the case of aerobic MBR (Di Bella et al. 2008; Lee et al. 2002; Zarragoitia-González et al. 2008; Zuthi et al. 2012), and only few have been proposed for the case of an AnMBR.

4

Developed for anaerobic digestion control and design, the Anaerobic Model AM2b is a simple model which involves only two main processes (methanogenesis and acidogenesis) and two bacterial populations in a two-step reactional framework (Benyahia et al. 2013). This model has the advantage of describing the dynamics of SMP within an anaerobic reactor such as its production during both methanogenesis and acidogenesis as well as during micro-organism decay, and their degradation by acidogens during acidogenesis. The AM2b model is then able to simulate the dynamics of major membrane foulants (microbial flocs and SMP).

This paper presents a complete model adapted to AnMBR control by coupling the AM2b model describing the biological treatment and a separation model describing membrane fouling. This combined model was validated by fitting both biological variables (TSS, COD and VFA) and TMP data, as well as cake deposit composition. The lack in the literature of comprehensive models able to simulate the combined effect of biological treatment and membrane fouling, which could be useful for AnMBR control, is behind the originality of this work. Moreover, the special feature of this model is that it allows the characterizations of the cake deposited on the membrane surface (SMP and Total Suspended Solids (TSS) contents) over time. The cake deposit composition is indeed very helpful in confirming model accuracy in order to define adapted membrane cleaning strategy.

2. Material and methods

2.1. AnMBR set-up

The AnMBR unit was set up as shown in Figure 1. The system detailed in Thongmak et al. (2015) consisted of the association of two reactors in series (reactor 1 as an anaerobic reactor and reactor 2 as a separation vessel), presenting a total volume of 12L (6L each reactor). The experiments were performed during two periods. During the first period, the start-up period, reactor 2 was only functioning as a settling step. During the second period, after day 75,

5

reactor 2 was equipped with a submerged hollow fiber PVDF membrane module (Shanghai Jofur Advanced Materials Co. Ltd, China) with a diameter of 0.7/1.3 mm (inner/outer), a total filtration area of 0.05m2 and a mean pore size of 0.1μm. The hydraulic resistance of the cleaned membrane measured at 27°C is $4.2*10^{11}$ (m^{-1}).
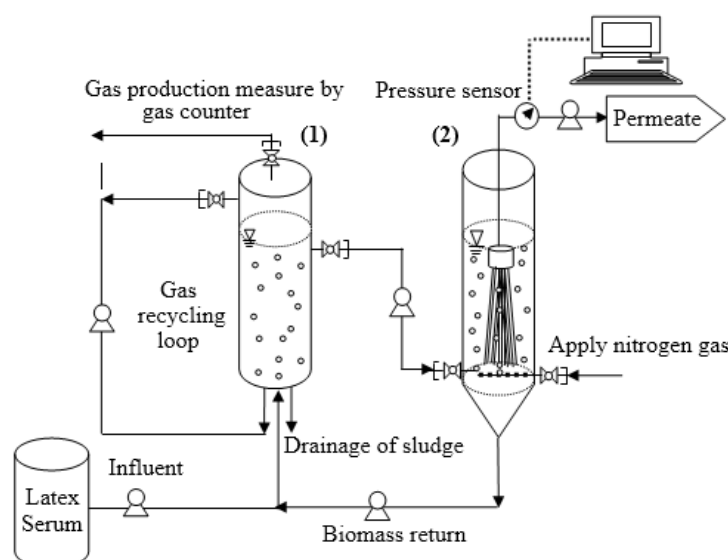
(1): Chamber 1-Anaerobic reactor   (2): Chamber 2-Membrane

Figure 1: Schematic diagram of AnMBR set-up

Common working conditions for the start-up period and the AnMBR period were considered. The temperature and pH were 30±2°C and 7±0.2, respectively. Influent COD, BOD$_5$ and NH$_3$-N concentrations were 16.2±0.4 (kg.m^{-3}), 7.6±0.4 (kg.m^{-3}) and 0.5±0.03 (kg.m^{-3}), respectively. The Feed, permeate and Waste flowrates were 0.246, 0.230 and 0.016 (L.h^{-1}), respectively. The Hydraulic and Solid retention times were 2 days and 30 days respectively. The organic loading rate was 8.1 (kgCOD.m^{-3}.d^{-1}).

2.2. Experimental conditions

The system was initially seeded by anaerobic sludge coming from the anaerobic digestion plant of a latex factory in the Songkhla province, South Thailand. The feed solution was a

6

latex serum obtained from a skim latex filtration (0.22 μm membrane cut off). The characteristics of this feed latex serum are detailed in Section 2.1.

This latex serum was a light yellow coloured solution with a low turbidity (absence of particular fraction due to its recovery by porous membrane filtration). The ratio COD/BOD_5 (2.13) confirms its significant degree of biodegradability.

The experimental set-up was operated under an organic loading rate (OLR) of 8.1 $kgCOD.m^{-3}.d^{-1}$. The experiment lasted 128 days based for the two periods, a start-up period and an AnMBR period. The initial sludge concentration in the bioreactors was $10 gVSS.L^{-1}$ and the pH was maintained in the range of 6.8-7.2 by the addition of sodium hydroxide (1N). During the AnMBR period (from day 75 to day 128). The filtration was operated by using a peristaltic pump connected to the permeate side of the membrane module. A pressure sensor was located in the permeate line in order to measure trans-membrane pressure (TMP). A computer with Lab-View application was connected to a data acquisition card (National Instruments, Austin, USA). The biogas production was evaluated by gas counter measurement. Biogas composition was analysed by gas chromatography (Agilent, Column-HP-PLOT Q).

To determine the soluble SMP concentration within the cake deposit, the fouled membrane module was rinsed with distilled water to remove compounds attached to the membrane surface. The rinsing water recovered from fouled membrane cleaning was centrifuged for 30 minutes at 2,360g. The supernatant from the centrifugation step was filtrated through a membrane with a mean pore size of 0.45 μm. The permeate of this last filtration step thus contained SMP fractions. The SMP concentration, considered as the sum of soluble proteins and carbohydrates,   was determined by the colorimetric method of Lowry et al. (1951) and Dubois et al. (1956), who used bovine serum albumin (BSA) and glucose as protein and carbohydrate standards, respectively.

To regenerate the membrane, chemical cleaning was used by soaking the membrane for 2h successively in 0.5v/v% sodium hydroxide solution, 0.5v/v% sodium hypochlorite solution and 0.5v/v% hydrochloric acid solution.

2. 3. Biological model

The biological model considered in this work to simulate the anaerobic biological system dynamics as well as its composition at steady state, is the Anaerobic Model AM2b (Benyahia et al. 2013). This model considers five state variables as shown in Figure 2, which are the acidogens (X_1), the methanogens (X_2), the COD (S_1) the volatile fatty acids (S_2) and the soluble microbial products (S). Moreover, 5 biological processes were assumed (Table 1). This model is able to estimate the bulk concentration of the two main foulants in the AnMBR which are (i) the total suspended solids (X_{TSS}) assumed as the total concentration of micro-organisms X_1 and X_2, and (ii) the soluble microbial products (S). The effect of those two components groups (particles and biopolymers) on membrane fouling scale will be highlighted in the fouling model presented in the next section (2.4).
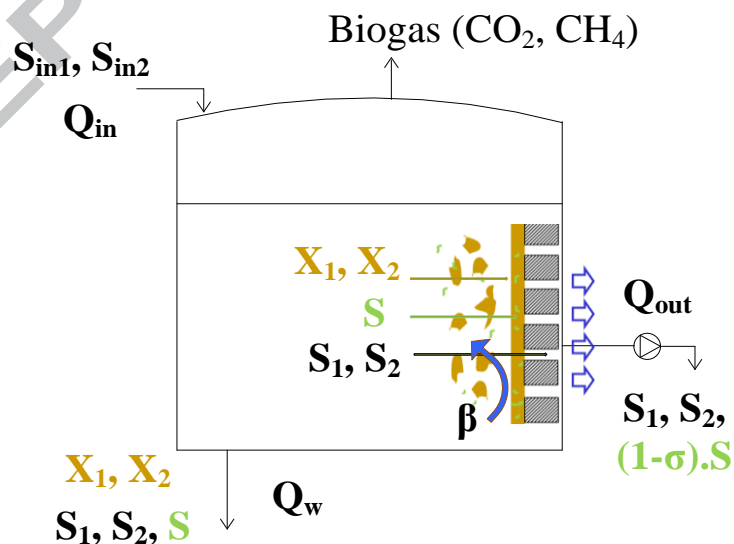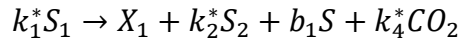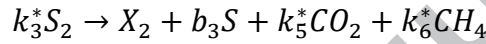

Figure 2: Schematic representation of AM2b and fouling combined model
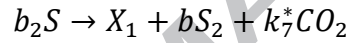
8

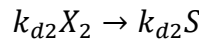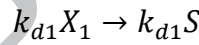Table 1: Reactions assumed in the AM2b model

Acidogenesis and SMP production

$$k_1^* S_1 \rightarrow X_1 + k_2^* S_2 + b_1 S + k_4^* CO_2$$

Methanogenesis and SMP production

$$k_3^* S_2 \rightarrow X_2 + b_3 S + k_5^* CO_2 + k_6^* CH_4$$

SMP degradation

$$b_2 S \rightarrow X_1 + b S_2 + k_7^* CO_2$$

SMP production during micro-organisms decline

$$k_{d1} X_1 \rightarrow k_{d1} S$$

$$k_{d2} X_2 \rightarrow k_{d2} S$$

Based on mass balance realized within the anaerobic reactor, the variation of the five state variables are expressed in Equations 1 to 5.

$$\frac{dX_1}{dt} = \left(\mu_1 + \mu_{smp} - k_{d1} - \frac{Q_w}{V_R}\right) X_1 \tag{Eq. 1}$$

$$\frac{dX_2}{dt} = \left(\mu_2 - k_{d2} - \frac{Q_w}{V_R}\right) X_2 \tag{Eq. 2}$$

$$\frac{dS_1}{dt} = \left(\frac{Q_{in}.S_{1in}}{V_R}\right) - \left(\left(\frac{Q_{out}}{V_R} + \frac{Q_w}{V_R}\right).S_1\right) - (k_1^*.\mu_1.X_1) \tag{Eq. 3}$$

$$\frac{dS_2}{dt} = \left(\frac{Q_{in}.S_{2in}}{V_R}\right) - \left(\left(\frac{Q_{out}}{V_R} + \frac{Q_w}{V_R}\right).S_2\right) - (k_3^*.\mu_2.X_2) + (k_2^*.\mu_1 + b.\mu_{smp})X_1 \tag{Eq. 4}$$

$$\frac{dS}{dt} = -\left((1-\sigma).\frac{Q_{out}}{V_R} + \frac{Q_w}{V_R}\right).S + (b_1.\mu_1 + k_{d1} - b_2.\mu_{smp}).X_1 + (b_3.\mu_2 + k_{d2}).X_2 \tag{Eq. 5}$$

9

As demonstrated in the literature (Benyahia et al. 2013; Bernard et al. 2001), the growth kinetic μ_1 of acidogens (X_1) by consuming COD (S_1) expressed in Equation 6, as well as the growth kinetic μ_{smp} of acidogens (X_1) by consuming SMP (S) expressed in Equation 8, are based on Monod function. However, the growth kinetic μ_2 of methanogens (X_2) by consuming VFA (S_2) expressed in Equation 7 is based on the Haldane function considering the inhibition effect on acidogens growth with a high VFA concentration.

$$\mu_1 = \mu_{\max 1} \cdot \frac{S_1}{K_1 + S_1} \qquad (Eq.\,6)$$

$$\mu_2 = \mu_{\max 2} \cdot \frac{S_2}{K_2 + S_2 + \frac{S_2^2}{K_i}} \qquad (Eq.\,7)$$

$$\mu_{smp} = \mu_{\max 3} \frac{S}{K_3 + S} \qquad (Eq.\,8)$$

2. 4. Fouling model

The proposed model considers the total suspended solids (TSS) referred to as (X_{TSS}) expressed in Equation 9 and the Soluble Microbial products (SMP) referred to as (S), as the two major foulant groups. While the suspended solids are totally rejected by the membrane barrier, only a fraction of the SMP, noted as σ, is retained by the membrane (Charfi et al. 2015). Rejected by the membrane barrier, both foulants (X_{TSS} and S) would deposit on the membrane surface and form a fouling layer, this phenomenon is called cake formation.

$$X_{TSS} = X_1 + X_2 \qquad (Eq.\,9)$$

with X_1 the acidogens concentration (kg.m^{-3}) and X_2 the methanogens concentration (kg.m^{-3}).

The cake formation is assumed to be the only mechanism controlling fouling in the AnMBR (Charfi et al. 2012; Waeger et al. 2010). As observed in the experiments conducted and confirmed in previous studies (Ognier et al. 2004; Saroj et al. 2008), when operating at constant flux, membrane fouling leads to TMP increase, which goes through two phases, a slow increase phase followed by a TMP jump.

Based on this observation, it has been assumed the cake formation is due to two mechanisms, (i) the deposition of suspended solids X_{TSS} to form the cake baseline which is responsible of the slow fouling and the slow TMP increase, and (ii) the introduction of the SMP in the cake's pores leading to decrease in the deposit porosity, responsible of the TMP jump. The model assumes that membrane fouling would start from the beginning of the filtration process.

The deposit mass m_c calculation, based on a mass balance realized on the membrane surface, is the difference between the mass of matter brought to the membrane surface, by convection flow forces and the mass of matter detached from the membrane surface by shear forces created by nitrogen bubbling (Eq.10).

$$\frac{dm_c}{dt} = Q_{out}.X_{TSS}.(1 - \beta m_c) \qquad (Eq.\,10)$$

with Q_{out} the permeate flowrate ($m^3.s^{-1}$), X_{TSS} the total micro-organisms concentration ($kg.m^{-3}$), β the shear parameter (kg^{-1}) and m_c the cake mass (kg).

The deposit's porosity decrease is assumed to be directly proportional to the amount of SMP (S) entrapped in the cake layer (Eq.11).

$$\frac{d\varepsilon}{dt} = -k_{\varepsilon}.\frac{Q_{out}}{A}.\sigma.S.\mathrm{E} \qquad (Eq.\,11)$$

$$\mathrm{E} = \frac{\varepsilon}{\varepsilon + \mathrm{n}} \qquad (Eq.\,12)$$

with k_{ε} the coefficient of deposit porosity decrease, Q_{out} the permeate flowrate ($m^3.s^{-1}$), A the membrane surface area (m^2), σ the SMP fraction retained by the membrane, S the SMP concentration ($kg.m^{-3}$) and ε the deposit porosity.

The function E expressed in Equation 12 is a mathematical expression used to avoid obtaining a negative value of deposit porosity. As the value of n was found to be equal to 10^{-14}, the E function is always equal to 1 and is not useful here.

The deposit's porosity decrease leads to a specific cake resistance increase expressed by the Kozeny-Carman equation (Eq.13) (Chudacek and Fane 1984). This phenomenon would be responsible for the increase in cake resistance, leading to the TMP jump (Charfi et al. 2015).

$$\alpha = \frac{180\,(1-\varepsilon)}{\rho_c d^2 \varepsilon^3} \qquad \qquad (Eq.\,13)$$

with ε the deposit porosity, ρ_c the deposit density (kg.m^{-3}), d the deposit particles diameter (m).

The theoretical values of TMP are then determined using a resistance in series model (Eq. 14).

$$TMP = \mu.(R_0 + R_c)\frac{Q_{out}}{A} \qquad \qquad (Eq.\,14)$$

with μ the permeate viscosity (Pa.s), R_0 the intrinsic membrane resistance (m^{-1}), R_c the deposit resistance (m^{-1}), Q_{out} the permeate flowrate (m^3.s^{-1}) and A the membrane surface area (m^2).

The deposit resistance is expressed as follows:

$$R_c = \alpha.\frac{m_c}{A} \qquad \qquad (Eq.\,15)$$

with α the specific deposit resistance (m.kg^{-1}), m_c the deposit mass (kg) and A the membrane surface area (m^2).

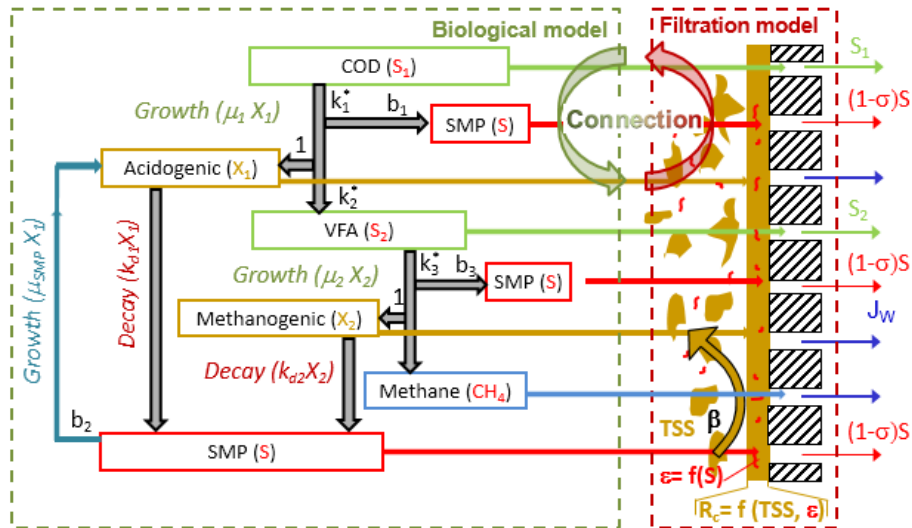The fouling and biological models have been combined as detailed in Figure 3.

12

Figure 3: Conceptual schema of the combined models

3. Results and discussion

To simulate the combined model, the equations were resolved sequentially, starting by the AM2b biological model equations followed by the fouling model equations. In fact the values of the total suspended solids (X_{TSS}) and SMP (S) at steady state simulated by the AM2b model were used as constants to simulate the fouling model. For model validation, we started by validating the biological model followed by the fouling model.

3. 1. Biological model validation

The Anaerobic Model AM2b has been validated using experimental data registered on the AnMBR setup shown in Figure 1. The experimental data related to the total micro-organisms' concentration measured as the total suspended solids concentrations (X_{TSS}) (Figure 4A) shows an increase with time and tends to a steady state value around 17g/L after 90days of experiment. Figure 4B and Figure 4C display the experimental concentrations with time of COD (S_1) and VFA (S_2), respectively. Those data show steady values around 2.3gCOD/L and $0.8_{gequivalent\ acetate}$/L, respectively. Even if it is considered as the simplest model describing an anaerobic biological system, numerous parameters are used in the AM2b model. For model

13

validation, the model parameters shown in Table 2 were fixed, based on experimental data and on the literature (Benyahia et al. 2013; Bernard et al. 2001), while the model parameters displayed in Table 3 were identified by the Least Squares method using Matlab software. This method is based on optimizing the model parameters permitting the minimization of the Least Squares (LS) function (Eq. 16).

$$LS = \sum (Experimental\ data - Simulation\ data)^2 \qquad \text{(Eq. 16)}$$

The model was then adjusted using the experimental data for total suspended solid concentration (X_{TSS}), the COD concentration (S_1), the VFA concentration (S_2) and the methane production. As shown in Figure 4A, the model accurately describes the total micro-organism growth with a coefficient of determination R^2 of 0.98. Moreover, the model which fits with the COD concentration (Figure 4B) as well as the VFA concentration (Figure 4C), shows satisfactory results during the stationary phase with an R^2 of 0.99 for both cases. The model is able to simulate the SMP concentration (S) within the bioreactor as displayed in Figure 4D. At steady state the SMP concentration is estimated at 0.8g.L^{-1}. This value will be used for the fouling model simulation and validation detailed in section 3.2.

Table 2: Biological model parameter values adopted from the literature (Benyahia et al. 2013; Bernard et al. 2001)

μ_{max1} (d^{-1})	μ_{max2} (d^{-1})	K_1 ($kg.m^{-3}$)	K_2 ($kg.m^{-3}$)	K_i ($kg.m^{-3}$)	σ (-)
0.252	0.132	7.1	0.54	15	0.5
k_1^* (-)	k_2^* (-)	k_3^* (-)	k_6^* (L_{CH4}/g_{COD})	kd_1 (d^{-1})	kd_2 (d^{-1})
11	15	16	2.49	$38.4*10^{-3}$	$38.4*10^{-3}$

Table 3: Biological model parameter values identified by the Least Squares method

μ_{max3} (d^{-1})	K (kg.m^{-3})	b (-)	b_1 (-)	b_2 (-)	b_3 (-)
0.12	15	0.6	2.5	50	1.3

A

B
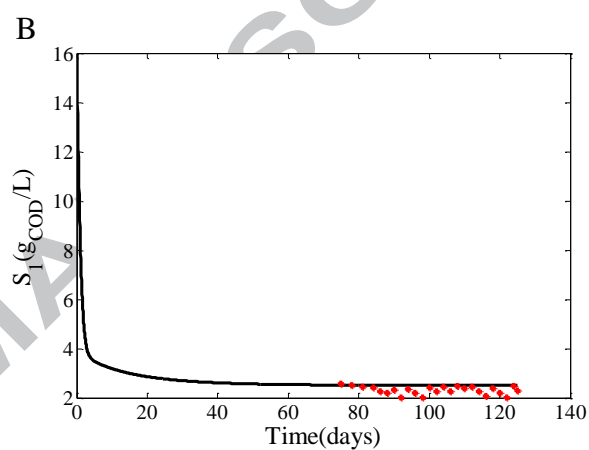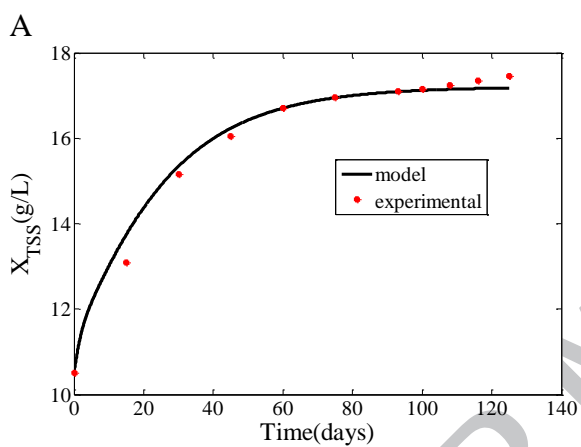
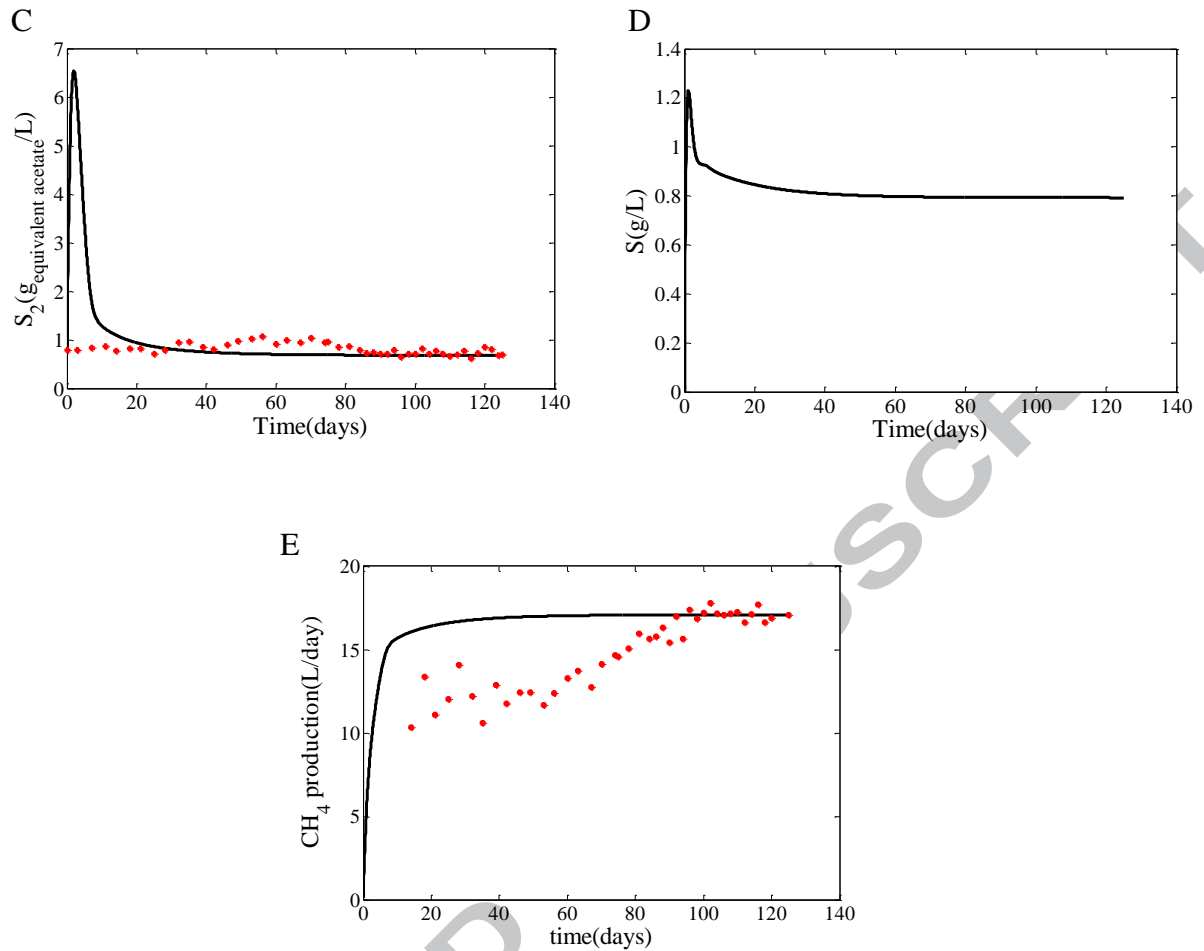Figure 4: Model fitting with the experimental data from the biological parameter (A) biomass growth, (B) COD data, (C) VFA data; (D) simulation of SMP concentration in the bulk; (E) Model fitting with the CH$_4$ production

The methane flowrate is assumed to be proportional to methanogen growth as expressed below:

$$\varphi_{CH_4} = k_6^* . \mu_2 . X_2 \qquad \text{(Eq. 17)}$$

Moreover, due to the low solubility of methane, the concentration of dissolved methane is neglected (Bernard et al. 2001). The concentration of methanogens at steady state, have been determined based on mass balance realized on COD concentration S$_1$ (Eq. 3) and VFA concentration S$_2$ (Eq. 4). The methane produced from SMP regeneration is assumed to be negligible (Bernard et al. 2001). The methane flowrate at steady state φ_{CH4} (mol$_{CH4}$.L^{-1}.day^{-1}), is then determined:

16

$$\varphi_{CH_4} = \frac{k_6^*}{k_3^*} \left(\left(\frac{k_2^*}{k_1^*} (S_{1in} - S_1) + S_{2in} \right) - S_2 \right) \frac{Q_{in}}{V_R} \qquad \text{(Eq. 18)}$$

Figure 4E shows the comparison of experimental data and model simulation for methane production. The discrepancy found between model simulation and the variation of methane production during the first 90 days is due mainly to neglecting methane solubility. Nevertheless the simulation of the steady state seems satisfactory after 90 days of experiment. Since this is based on the consumption of the organic matter present in the influent for biogas production, this model is likely to deal with all organic pollutants and not only serum latex influent.

3. 2. Fouling model validation

The fouling model has been validated using experimental TMP data obtained on the AnMBR set up shown in Figure 1. TMP data have been recorded during 3 successive filtration cycles, under similar operating conditions and separated by chemical cleaning (Figure 5A). During those three filtrations cycles TMP increase goes through two phases: (i) a first phase of slow increase during the first 6 hours of filtration followed by (ii) a second phase of TMP jump. The first cycle data were used to identify two model parameters, (i) the shear parameter β and (ii) the coefficient of deposit porosity decrease k_ε. The parameter identification was realized by adjusting the fouling model on the first TMP cycle data (Figure 5B) using the Least Squares (LS) method on Matlab software based on the minimization of the LS function (Eq. 16)

The values obtained for identified parameters as well as the fixed values of other parameters are displayed in Table 4. The model fitted well with the first cycle data with a coefficient of determination R^2 of 0.89 (Figure 5B). The values of parameters identified while fitting the model with the first cycle TMP data, were used to predict the TMP data of the second and third filtration cycles. The model fitted well with the experimental data with R^2 of 0.94 and

0.83 respectively (Figures 5C and 5D). The proposed model seems effective to predict TMP variation in an AnMBR.
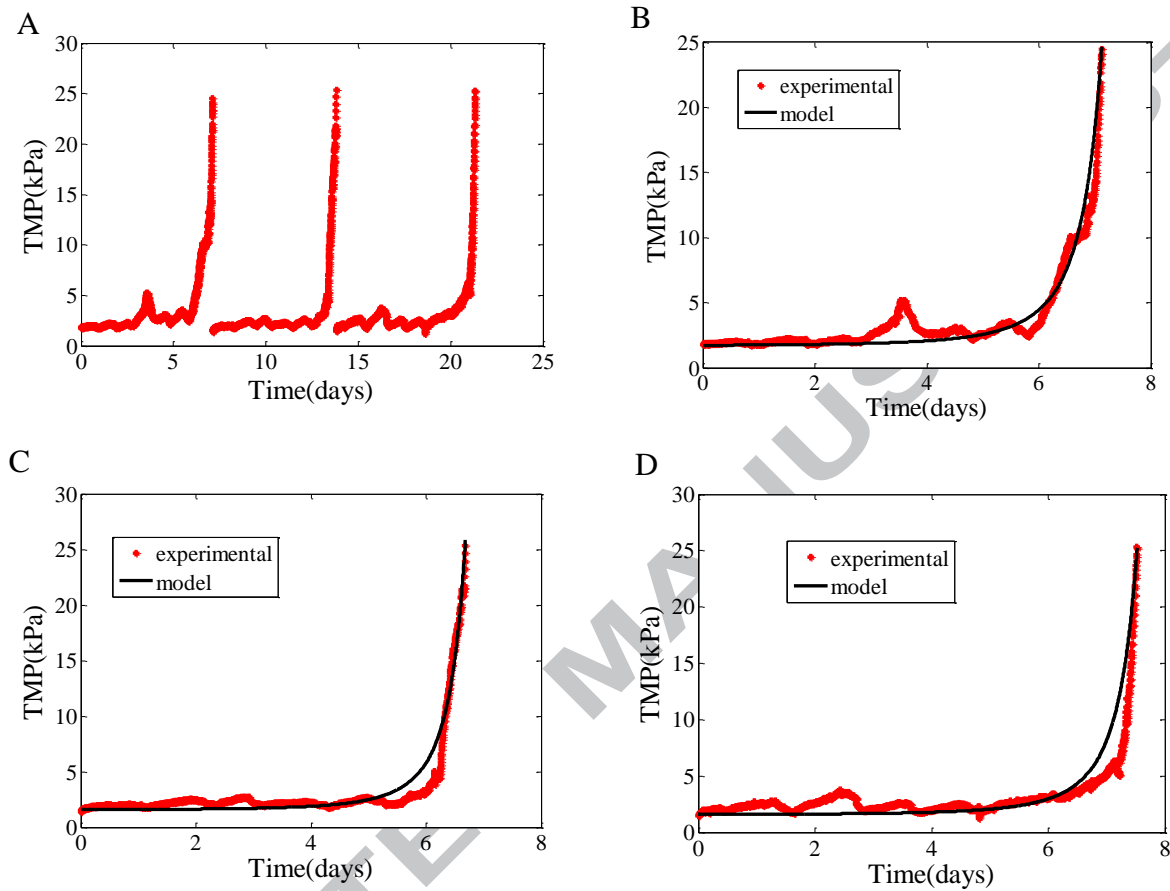

Figure 5: (A) experimental values of TMP for 3 filtration cycles separated by a chemical cleaning; Model adjustment on TMP data (B) for the 1st filtration cycle, (C) for the 2nd filtration cycle (D) for the 3rd filtration cycle.

Table 4: Fouling model parameters

Fixed parameters		
Membrane surface area	$A\ (m^2)$	0.05
Permeate viscosity	$\mu_p\ (Pa.s)$	0.001
SMP	$S\ (kg.m^{-3})$	0.8
SMP rejection	σ	0.5
MLVSS	$X_{TSS}\ (kg.m^{-3})$	17.5
Permeate flowrate	$Q_{out}\ (L.h^{-1})$	0.23

18

Membrane initial resistance	R_m (m^{-1})	$4.2*10^{11}$
Deposit particle diameter	d (m)	$30*10^{-6}$
Empirical constant	n	10^{-14}
Initial deposit porosity	ε_0	0.4
Deposit density	ρ_c (kg.m^{-3})	10^3
SMP density	ρ_{smp} (kg.m^{-3})	$1.32*10^3$
Optimized parameters		
Coefficient of deposit porosity decrease	k_ε	$1.1*10^{-3} \pm 0.003$
Shear parameter	β (g^{-1})	2.5 ± 0.05

3. 3. Deposit mass composition

In this paper, a new tool was proposed to determine the composition of the deposited cake. This allows both deposit mass and SMP content within this deposit to be predicted. The deposit is indeed composed by flocs and SMP entrapped on the membrane surface according to convective flux, membrane rejection and detachment (see section 2.4). For this purpose, the deposit mass and SMP entrapped on the membrane must be recorded (Eqs. 19 and 22).

Based on Equation 10, we proposed Equation 19 to determine the mass of suspended solid (m_X) deposited according to the first fouling mechanism.

$$\frac{dm_X}{dt} = \frac{Q_{out}}{A} . X_{TSS} . (1 - \beta . m_c) \qquad (Eq. 19)$$

Then V_c, expressed in Equation 20, is defined as the deposit volume (m^3).

$$V_c = m_c / \rho_c \qquad (Eq. 20)$$

The mass of SMP accumulated within the deposit due to the second fouling mechanism, is determined based on Equation 11 which expresses the decrease of deposit porosity by SMP

19

(dε/dt). The deposit porosity decrease is proportional to the volume of SMP (V_S) trapped within the deposit pores as expressed below:

$$\frac{1}{V_c}\frac{dv_S}{dt} = \left|\frac{d\varepsilon}{dt}\right| = k_\varepsilon.\frac{Q_{out}}{A}.\sigma.S.\frac{\varepsilon}{\varepsilon+n} \qquad \text{(Eq. 21)}$$

The mass variation of SMP trapped within the deposit m_s is expressed by equation 22.

$$\frac{dm_s}{dt} = \rho_{smp}.\frac{d_{V_S}}{dt} \qquad \text{(Eq. 22)}$$

with ρ_{smp} the SMP density (kg.m^{-3}) and Vs the volume of SMP trapped within the deposit (m^3).

By combining Equations 20, 21 and 22, the variation of SMP mass (m_S) accumulated within the deposit according to the second mechanism is expressed as:

$$\frac{dm_s}{dt} = \frac{\rho_{smp}}{\rho_c}.\frac{Q_{out}}{A}.m_c.k_\varepsilon.\sigma.S.\frac{\varepsilon}{\varepsilon+n} \qquad \text{(Eq. 23)}$$

Based on the parameter values in Table 4, the simulation of deposit composition during the first filtration cycle is presented in Figure 6A. The simulations show the specific mass of suspended solids entrapped on the membrane (m_X) due to the first fouling mechanism, which increases quickly to reach a constant value within 5h of filtration. Figure 6A also displays the specific mass of SMP (m_S) deposited due to the second fouling mechanism. The parameter m_S keeps increasing, and reaches a constant value when deposit porosity reaches equilibrium (dε/dt=0). After 7 days of filtration the deposit is composed of 7.7g.m^{-2} of micro-organisms flocs and 4.5g.m^{-2} of SMP which represent 63.1% and 36.9% of the total deposit specific mass, respectively (Fig. 6A). The simulated value of SMP specific mass of m_S deposited within 7days of filtration, is similar to the value measured experimentally (Thongmak et al., 2015) which is ≈4.2g.m^{-2}. This shows the accuracy of the proposed model. X_{TSS} leads to a

20

rapid creation of the cake layer (within 5 hours) without impacting significantly the transmembrane pressure, whereas the entrapment of SMP in the deposit, leads to a continuous decrease of the deposit porosity (Fig. 6B), which triggers the TMP jump.
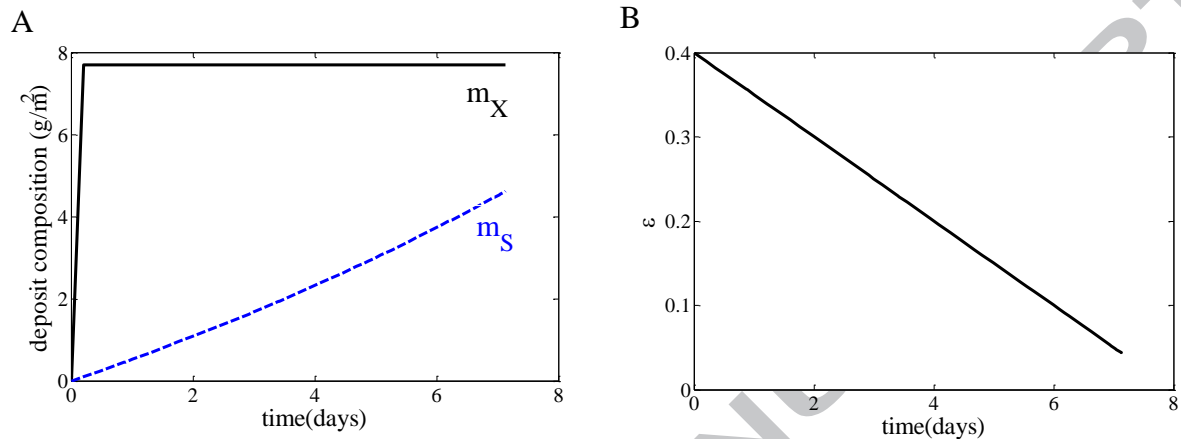

Figure 6: (A) Deposit composition determined for the first filtration cycle, (B) Model simulation of the decrease of deposit porosity

The proposed model was shown to be effective to simulate, for a fixed experimental conditions of HRT and SRT as well as a fixed COD concentration of wastewater to treat, the biological system dynamics, the fouling development through TMP increase, the methane gas production and the deposit composition in terms of SMP and suspended solids. This model could be then a useful tool to optimize the operating conditions, for different wastewaters treatment, based on their COD concentration, to foster methane production and control membrane fouling in an AnMBR. Furthermore it would be useful to determine an effective strategy of membrane cleaning for an optimal process productivity.

4. Conclusion

This paper presented a simple model combining filtration and AM2b biological models, to study the impact of biological parameters on membrane fouling in an AnMBR. While the biological model accurately described the total suspended solid concentration, the COD, the VFA and the biogas production within the anaerobic reactor at the steady state ($R^2 \approx 0.99$), the

21

filtration model fitted well with TMP experimental data ($R^2 \approx 0.90$). This notion of a complete model demonstrates an interconnection between both biological and filtration fields and is an efficient model for quantifying membrane fouling due to cake deposition in an AnMBR in order to estimate biogas production.

Acknowledgements

References

1. Abdelrasoul, A., Doan, H., Lohi, A., 2013. A mechanistic model for ultrafiltration membrane fouling by latex. J. memb. sci. 433, 88-99.
2. Aslam, M., McCarty, P. L., Shin, C., Bae, J., Kim J., 2017. Low energy single-staged anaerobic fluidized bed ceramic membrane bioreactor (AFCMBR) for wastewater treatment. Bioresour. Technol. 240, 33-41
3. Aslam, M., McCarty, P.L., Bae, J., Kim, J., 2014. The effect of fluidized media characteristics on membrane fouling and energy consumption in anaerobic fluidized membrane bioreactors. Sep. Purif. Technol. 132, 10-15.
4. Aslam, M., Charfi, A., Lesage, G., Heran, M., Kim, J., 2017. Membrane bioreactors for wastewater treatment: A review of mechanical cleaning by scouring agents to control membrane fouling. Chem. Eng. J. 307, 897-913.
5. Benyahia, B., Sari, T., Cherki, B., Harmand, J., 2013. Anaerobic membrane bioreactor modeling in the presence of soluble microbial products (SMP)–the anaerobic model AM2b. Chem. Eng. J. 228, 1011-1022.
6. Bernard, O., Hadj-Sadok, Z., Dochain, D., Genovesi, A., Steyer, J. P., 2001. Dynamical model development and parameter identification for an anaerobic wastewater treatment process. Biotechnol. bioeng. 75, 424-438.
7. Charfi, A., Ben Amar, N., Harmand, J., 2012. Analysis of fouling mechanisms in anaerobic membrane bioreactors. Water Res. . 46, 2637-2650.

8. Charfi, A., Harmand, J., Ben Amar N., Grasmick, A., Héran, M., 2014. Deposit membrane fouling: influence of specific cake layer resistance and tangential shear stresses. Water Sci. Technol. 70, 40-46.

9. Charfi, A., Yang, Y., Harmand, J., Ben Amar, N., Heran, M., Grasmick, A., 2015. Soluble microbial products and suspended solids influence in membrane fouling dynamics and interest of punctual relaxation and/or backwashing. J. Memb. Sci. 475, 156-166.

10. Charfi, A., Aslam, A., Lesage, G., Heran, M., Kim, J., 2017. Macroscopic approach to develop fouling model under GAC fluidization in anaerobic fluidized bed membrane bioreactor. J. Ind. Eng. Chem. 49, 219-229.

11. Chudacek, M. W., Fane, A. G., 1984. The dynamics of polarisation in unstirred and stirred ultrafiltration. J. memb. sci. 21, 145-160.

12. Di Bella, G., Mannina, G., Viviani, G., 2008. An integrated model for physical-biological wastewater organic removal in a submerged membrane bioreactor: Model development and parameter estimation. J. Memb. Sci. 322, 1-12.

13. Dubois, M., Gilles, K.A., Hamilton, J.K., Rebers, P., Smith, F., 1956. Colorimetric method for determination of sugars and related substances. Anal. chem. 28, 350-356.

14. Hermia J, 1982. Constant pressure blocking filtration law application to powder-law non-Newtonian fluids. Trans. Inst. Chem. Eng. 60, 183-187.

15. Ho. J., Sung, S., 2009. Effects of solid concentrations and cross-flow hydrodynamics on microfiltration of anaerobic sludge. J. Memb. Sci. 345, 142-147.

16. Lee, Y., Cho, J., Seo, Y., Lee, J. W., Ahn, K.H., 2002. Modeling of submerged membrane bioreactor process for wastewater treatment. Desal. 146, 451-457.

17. Lowry, O. H., Rosebrough, N. J., Farr, A. L., Randall, R. J., 1951. Protein measurement with the Folin phenol reagent. J. biol. Chem. 193, 265-275.

18. Meng, F. Chae, S. R., Drews, A., Kraume, M., Shin, H. S., Yang, F., 2009. Recent advances in membrane bioreactors (MBRs): Membrane fouling and membrane material. Water Res. 43, 1489-1512.

19. Ognier, S., Wisniewski, C., Grasmick, A., 2004. Membrane bioreactor fouling in sub-critical filtration conditions: a local critical flux concept. J. Memb. Sci. 229, 171-177.

20. Pan, J. R., Su, Y.C., Huang, C., Lee, H. C., 2010. Effect of sludge characteristics on membrane fouling in membrane bioreactors. J. memb. Sci. 349,287-294.

21. Saroj, D. P., Guglielmi, G., Chiarani, D., Andreottola, G. 2008. Subcritical fouling behaviour modelling of membrane bioreactors for municipal wastewater treatment: The prediction of the time to reach critical operating condition. Desal. 231,175-181.

22. Smith, A. L., Stadler, L. B., Love, N. G., Skerlos, S. J., Raskin, L., 2012. Perspectives on anaerobic membrane bioreactor treatment of domestic wastewater: A critical review. Biores. Technol. 122, 149-159.

23. Thongmak, N., Sridang, P., Puetpaiboon, U., Héran, M., Lesage, G., Grasmick, A., 2016. Performances of a submerged anaerobic membrane bioreactor (AnMBR) for latex serum treatment. Desal. Water Treat. 57, 20694-20706.

24. Waeger, F., Delhaye, T., Fuchs, W. 2010. The use of ceramic microfiltration and ultrafiltration membranes for particle removal from anaerobic digester effluents. Sep. Purif. Technol. 73, 271-278.

25. Wang, W., Yang, Q., Zheng, S., Wu, D. 2013. Anaerobic membrane bioreactor (AnMBR) for bamboo industry wastewater treatment. Biores. Technol. 149, 292-300.

26. Wu, J., He, C., Jiang, X., Zhang, M., 2011. Modeling of the submerged membrane bioreactor fouling by the combined pore constriction, pore blockage and cake formation mechanisms. Desal. 279, 127-134.

27. Xia, T., Gao, X., Wang, C., Xu, X., Zhu, L. 2016. An enhanced anaerobic membrane bioreactor treating bamboo industry wastewater by bamboo charcoal addition: Performance and microbial community analysis. Biores. Technol. 220, 26-33.

28. Zarragoitia-González, A., Schetrite, S., Alliet, M., Jáuregui-Haza, U., Albasi, C. 2008. Modelling of submerged membrane bioreactor: conceptual study about link between activated slugde biokinetics, aeration and fouling process. J. Memb. sci. 325, 612-624.

29. Zuthi, M. F. R, Ngo, H. H, Guo, W. S.,2012. Modelling bioprocesses and membrane fouling in membrane bioreactor (MBR): A review towards finding an integrated model framework. Biores. Technol. 122, 119-129.

30. Zuthi, M. F. R., Guo, W. S., Ngo, H. H., Nghiem, D. L., Hai, F. I., Xia, S., Li, J., Liu, Y. 2017. New and practical mathematical model of membrane fouling in an aerobic submerged membrane bioreactor. Biores. Technol. 238, 86-94.

Highlights

- A model has been proposed to simulate fouling in an anaerobic membrane bioreactor.

- The proposed model is able to simulate the major foulants concentrations in the AnMBR.

- A numerical tool has been developed to determine the deposit cake composition.

- The Transmembrane pressure jump is due to a decrease in cake porosity.

Graphical abstract